Canadian Mineralogist
Vol. 29, pp. 481-498

BARIAN FELDSPAR AND BARIAN-CHROMIAN MUSCOVITE FROM THE HEMLO AREA, ONTARIO

YUANMING PAN AND MICHAEL E. FLEET
Department of Geology, University of Western Ontario, London, Ontario N6A 5B7

ABSTRACT

Green mica schists occur in close association with a barite-rich unit in the late Archean Hemlo - Heron Bay greenstone belt, approximately 21 km west of the Hemlo gold deposit, Ontario. They are characterized by anomalously high whole-rock Ba, Cr and Ti contents and minerals of unusual compositions. Feldspars include Ba-rich feldspar (celsian), ternary (Ba-K-Na) and (K-Ba-Na) feldspar with minor amounts of Sr (up to 0.6 wt. % SrO), Ba-poor alkali feldspar and microcline and exhibit three compositional discontinuities at Cn_{15-25}, Cn_{30-40} and Cn_{47-65}. The green mica contains high contents of Ba and Cr (up to 10.3 wt. % BaO and 6.4 wt. % Cr_2O_3) and, occasionally, Ti (up to 5.8 wt. % TiO_2) as well. Other minerals present are zincian-manganoan chromite (up to 8.9 wt. % ZnO and 13 wt. % MnO), chromian dravite (up to 9.8 wt. % Cr_2O_3), chromian rutile (up to 2.0 wt. % Cr_2O_3), spessartine-rich almandine, F-rich phlogopite, chlorite, titanite, fluorite, sulfides, and carbonates. Salient mineralogical and geochemical characteristics, along with field relations and textural evidence, indicate that these green mica schists were derived from a mafic-ultramafic precursor(s) by extensive hydrothermal alteration; the barian was derived from an adjacent barite-rich unit. The estimated conditions of crystallization, 530°C and 3-4 kbar, indicate that the main mineral assemblage formed during the waning stage of regional thermal metamorphism. Veins of F-rich phlogopite, calcite, and fluorite, formed during a late alteration at 300-330°C, 1 kbar by a moderately saline, high-$X(CO_2)$ fluid.

Keywords: barian feldspar, barian-chromian muscovite, barite occurrence, Hemlo, Ontario.

SOMMAIRE

Nous trouvons des schistes à mica vert étroitement liés à une unité riche en barite dans la ceinture de roches vertes archéenne de Hemlo - Heron Bay, environ 21 km à l'ouest du gisement d'or de Hemlo, en Ontario. Ces roches contiennent des concentration anormales de Ba, Cr et Ti, et des minéraux à compositions étrange. Le feldspath peut être soit riche en Ba (celsian, Cn), soit ternaire (Ba-K-Na et K-Ba-Na) avec faibles concentrations en Sr (jusqu'à 0.6% de SrO en poids), soit un feldspath alcalin à faible teneur en Ba, soit un microcline. Nous reconnaissons trois discontinuités dans la composition du feldspath, dans les intervalles Cn_{15-25}, Cn_{30-40} et Cn_{47-65}. Le mica vert contient des teneurs élevées de Ba, de Cr (jusqu'à 10.3% de BaO et 6.4% de Cr_2O_3, par poids), et même, plus rarement, de Ti (jusqu'à 5.8% de TiO_2). Sont aussi présents chromite zincifère et manganifère (jusqu'à 8.9% de ZnO et 13% en MnO), dravite chromifère (jusqu'à 9.8% de Cr_2O_3), rutile chromifère (jusqu'à 2.9% de Cr_2O_3), almandin riche en Mn, phlogopite riche en fluor, chlorite, titanite, fluorite, sulfures et carbonates. Les caractéristiques minéralogiques et géochimiques importantes, ainsi que les relations de terrain et les textures, concordent avec une origine de ces schistes par lessivage important d'un précurseur mafique ou ultramafique; par contre, le Ba a son origine dans l'unité adjacente riche en baryum. Les conditions de cristallization (530°C, 3-4 kbar) indiquent que l'assemblage principal se serait formé vers la fin d'un épisode de métamorphisme régional. Une paragenèse de phlogopite riche en fluor, calcite et fluorite, présente dans les fissures, représenterait un stade tardif d'altération à 300-330°C et 1 kbar, en présence d'une phase fluide à salinité moyenne et $X(CO_2)$ élevé.

(Traduit par la Rédaction)

Mots-clés: feldspath baryfère, muscovite baryfère et chromifère, barite, Hemlo, Ontario.

INTRODUCTION

Green mica schists and barite-rich rocks occur sporadically throughout the Hemlo - Heron Bay greenstone belt of Ontario (Patterson *et al.* 1983, Cameron & Hattori 1987). They are two important ore-bearing rocks in the Hemlo gold deposit, which hosts the three largest gold mines in current production in Canada and contains a total published reserve of approximately 80 million tonnes at an average grade of 7.7 g/t Au (Harris 1989). In the past few years, considerable attention (Patterson *et al.* 1983, Cameron & Hattori 1985, 1987, Roach *et al.* 1986) has been given to the barite-rich rocks because of their potential for industrial barite, and the association of barite with gold in the deposit; furthermore, such rocks represent the first occurrence of Archean barite to be documented in Canada. Although the mineralogy and geochemistry of green mica schists at

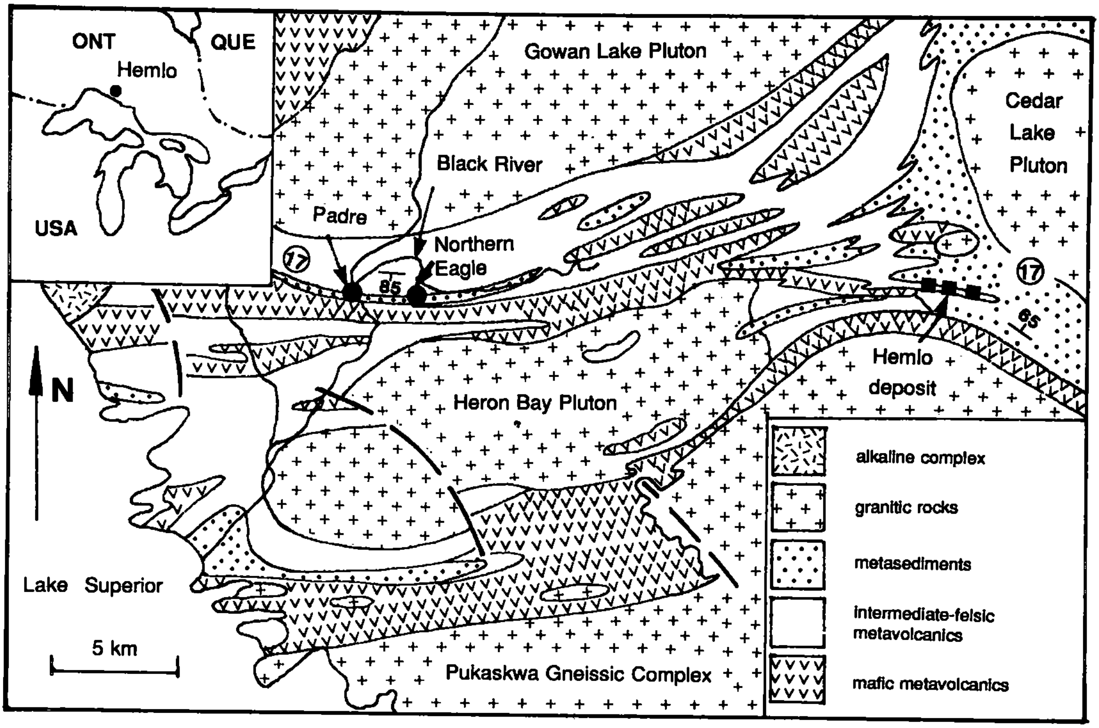

FIG. 1. Geological map of the barite occurrences (solid circles) and the Hemlo gold deposit (solid squares, after Muir 1982a, b).

Hemlo have been described by Harris (1989), green mica schists beyond the deposit generally remain uncharacterized. The green mica is a 2*M* vanadian muscovite that contains up to 8.5 wt.% V_2O_3 (Harris 1989). For many geologists working in the region, all occurrences of green mica from this greenstone-belt terrane are assumed to be vanadian muscovite and therefore are used as an important exploration indicator for gold mineralization.

This paper describes green mica schists from barite occurrences 21 km west of the Hemlo deposit. Their characteristic mineral association includes feldspar of the alkali feldspar - hyalophane - celsian series, (titaniferous) barian-chromian muscovite, and zincian-manganoan chromite. We present textural and chemical evidence to demonstrate that these green mica schists formed by extensive hydrothermal alteration during the complex evolution of the Hemlo - Heron Bay greenstone belt.

GEOLOGICAL SETTING

The barite occurrences, located approximately 21 km west of the Hemlo gold deposit, near the Black River bridge on Trans-Canada Highway 17 (Fig. 1), are situated within the Archean Hemlo - Heron Bay greenstone belt, which is part of the east-trending Schreiber - White River belt of the Wawa subprovince of the Superior Province (Muir 1982a, b). The geology of the Hemlo - Heron Bay greenstone belt, and particularly that of the mineralized Hemlo area, has been described by a number of authors: *e.g.*, Muir (1982a, b), Brown *et al.* (1985), Macdonald (1986), Patterson *et al.* (1983), Muir & Elliott (1987), Corfu & Muir (1989a, b), Harris (1989), Pan & Fleet (1990), and White & Barnett (1990). Most of these authors agree that the Hemlo - Heron Bay greenstone belt has been subjected to a complicated history of deposition, deformation, magmatism, metamorphism, and alteration. Metamorphic conditions are estimated to have been about 6 kbar and 500°C for an early Barrovian-type regional metamorphism. A regional thermal metamorphism, responsible for the penetrative foliation of the region and the main mineral assemblages of most supracrustal rocks, peaked at about 4 kbar and 580 ± 20°C; a late episode of low- to very-low-grade calc-silicate alteration, leading to abundant epidote–prehnite veins, overprinted the rocks at about 1.5 kbar and 350°C (Pan & Fleet 1990).

The barite occurrences west of the Hemlo deposit consist of a barite-rich unit and green mica,

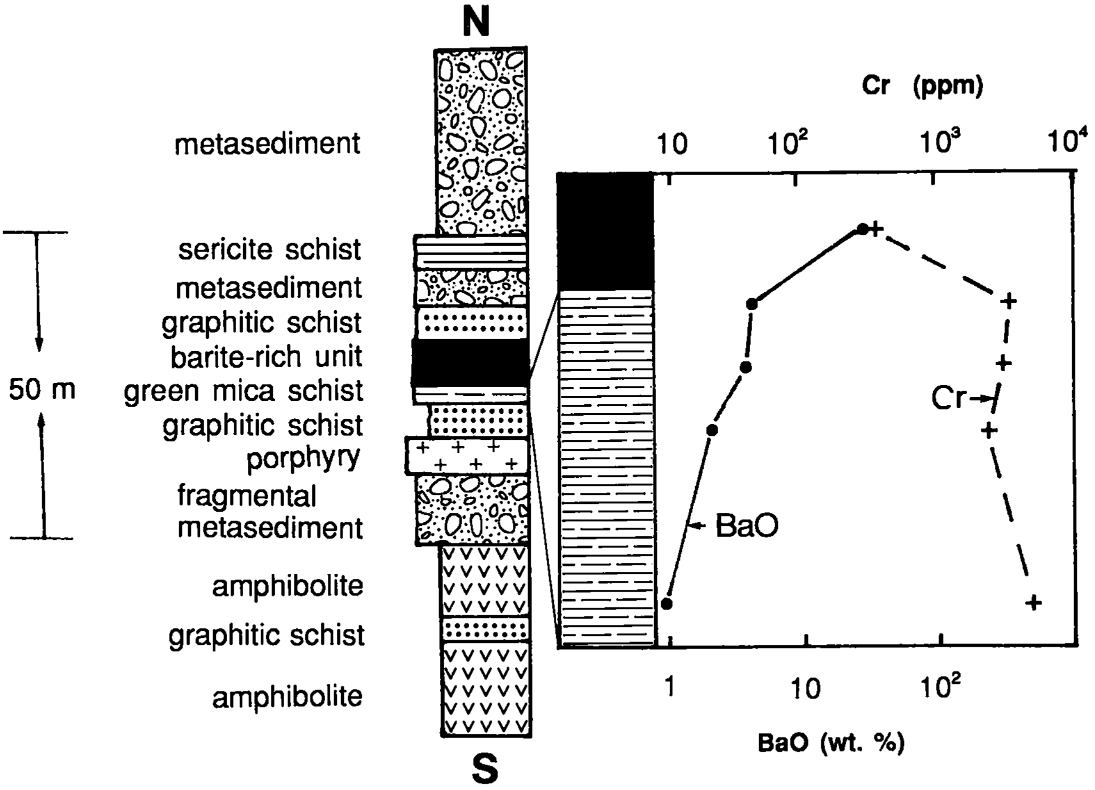

FIG. 2. Stratigraphy of the barite occurrence (after Patterson *et al.* 1983). Data on Ba and Cr contents of green mica schists and the barite-rich unit were determined on samples from the study area.

graphitic and sericite schists; these rocks occur as a conformable zone up to 50 m thick (Fig. 2) and can be traced by geology and geophysics for 6 km (Patterson *et al.* 1983). On a regional scale, the barite occurrences are structurally underlain by younger metasedimentary rocks to the north and structurally overlain by older mafic metavolcanic rocks to the south (Figs. 1, 2). The barite-rich unit has a strike of 110° and a vertical to steep southerly dip, and is characterized by well-developed layering defined by alternating barite-rich, feldspathic, and pyritiferous layers. In field exposures, the distinct emerald color of the green mica schists is even more spectacular, because of their association with layers of black graphitic schist and white sericite schist. Graphitic and sericite schists are volumetrically more abundant than the green mica schist in the study area, and appear to be more widespread in the Hemlo – Heron Bay greenstone belt. Locally, actinolite–chlorite–phlogopite–(talc) schist and biotite amphibolites are abundant within the green mica schists, and appear to be relict fragments of mafic–ultramafic rocks.

The structurally underlying metasedimentary rocks are strongly foliated, medium- to coarse-grained quartz–feldspar–biotite schists. Mineral assemblages consisting of garnet, staurolite, andalusite and kyanite also are exposed locally in metapelitic rocks, indicative of metamorphism in the low- to middle-amphibolite facies (Patterson *et al.* 1983). The structurally overlying mafic metavolcanic rocks are strongly foliated and locally garnetiferous amphibolites, but contain ellipsoidal relict pillows. This unit can be traced for several kilometers and may be a lateral extension of pillowed amphibolites south of the Hemlo deposit (Muir & Elliott 1987). The chemical compositions of garnet and hornblende in garnet amphibolites indicate metamorphic conditions at 570°C and 3.5 kbar according to the geothermometer of Graham & Powell (1984) and the geobarometers of Kohn & Spear (1990). These conditions are in good agreement with P–T estimates for the peak regional thermal metamorphism elsewhere in the Hemlo – Heron Bay greenstone belt (Pan & Fleet 1990).

ANALYTICAL PROCEDURES

Samples were collected mainly from two trenches on the Padre Resources Ltd. property, with additional diamond-drill core material from the Northern Eagle Mines Ltd. property (Goad 1987; Fig. 1). Selected mineral grains were analyzed on a JEOL JXA-8600 Superprobe with standard

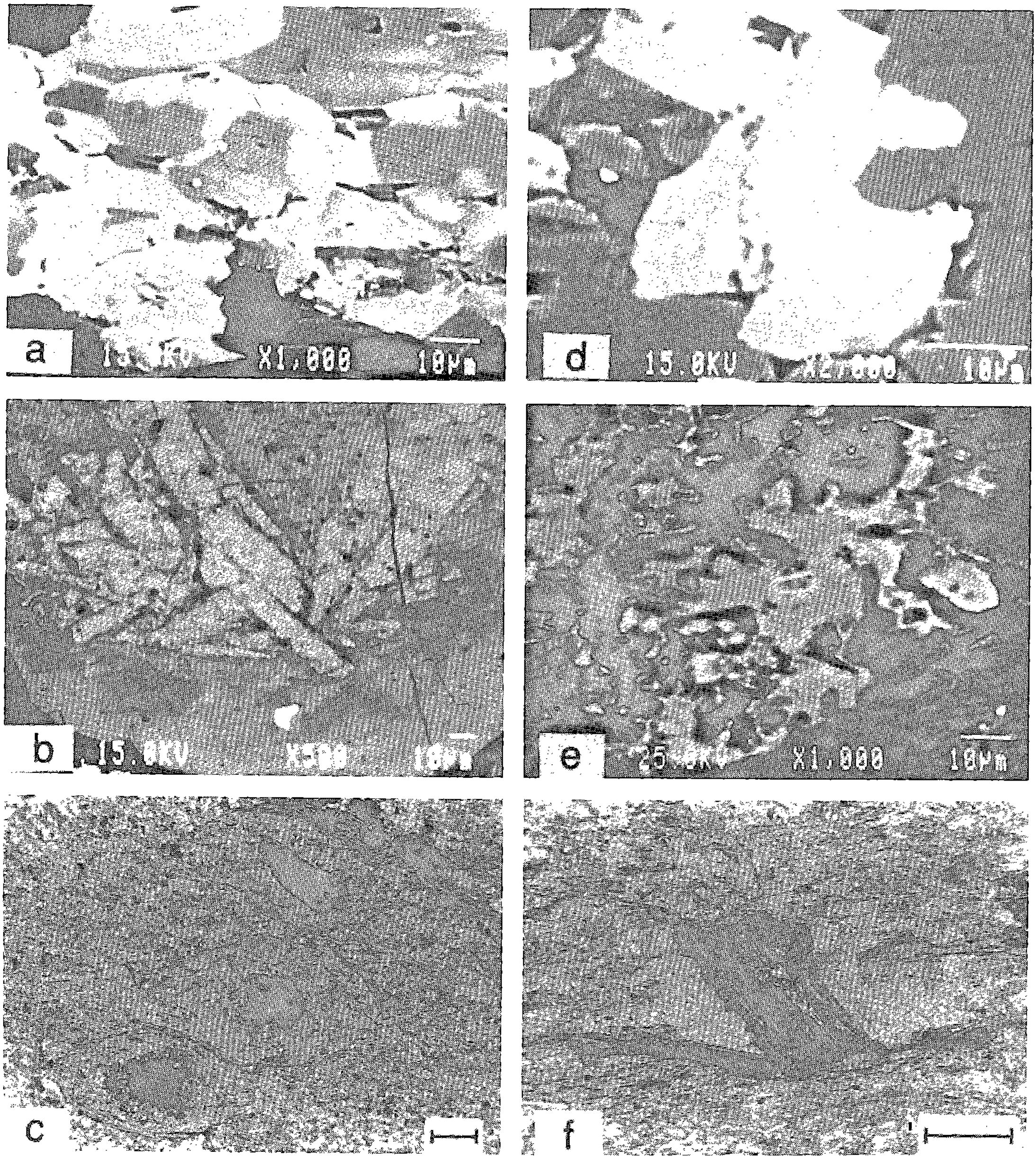

FIG. 3. Textural relationships (c and f are photomicrographs, scale bars are 0.05 mm; a, b, d, and e are electron back-scattered images): a) compositional zonation in barian feldspar from the barite-rich unit (grey core, Ba–K–Na ternary feldspar; bright margin, celsian); b) grains of homogeneous celsian from the barite-rich unit; c) muscovite after chromite porphyroblasts; d) compositional zonation in muscovite (Cr-rich, Ba-poor white core; Cr-poor, Ba-poor intermediate zone; Cr-poor, Ba-rich white margin); e), titaniferous muscovite after rutile; f) phlogopite along foliation planes.

TABLE 1. CHEMICAL COMPOSITION OF FELDSPARS

Sample	PR-1c	PR-1m	PR-2c	PR-2m	PRBUc	PRBUr	PRBUr	NE-1c	NE-1m	PR-5
SiO_2	64.31	59.24	53.78	48.32	47.00	40.84	33.40	63.93	60.37	58.73
Al_2O_3	18.51	19.91	21.36	22.26	23.53	25.25	27.38	18.15	19.63	26.08
CaO	nd	nd	nd	0.06	nd	0.05	nd	nd	nd	7.77
BaO	1.34	6.66	15.08	22.41	22.56	29.43	39.10	0.43	5.34	nd
SrO	nd	nd	0.60	nd	0.50	nd	nd	0.09	0.10	0.37
Na_2O	0.19	0.17	1.75	1.31	1.15	0.74	0.10	0.12	0.20	7.34
K_2O	16.15	14.19	8.16	6.01	6.14	3.56	0.32	16.79	14.56	nd
Total	100.5	100.2	100.7	100.4	100.9	99.87	100.3	99.51	100.2	100.3
Chemical formulae calculated on the basis of 8 oxygen atoms										
Si	2.985	2.864	2.716	2.579	2.510	2.319	2.041	2.991	2.890	2.621
Al	1.013	1.134	1.271	1.400	1.481	1.690	1.973	1.001	1.108	1.372
Ca	0.000	0.000	0.000	0.004	0.000	0.003	0.000	0.000	0.000	0.371
Ba	0.024	0.126	0.299	0.470	0.472	0.655	0.937	0.008	0.100	0.000
Sr	0.000	0.000	0.018	0.000	0.015	0.000	0.000	0.002	0.003	0.010
Na	0.017	0.016	0.166	0.135	0.119	0.081	0.012	0.011	0.019	0.635
K	0.956	0.874	0.527	0.410	0.418	0.258	0.025	1.001	0.889	0.000
Ab	1.7	1.6	16.4	13.2	11.6	8.1	1.2	1.1	1.9	62.5
An	0.0	0.0	0.0	0.4	0.0	0.3	0.0	0.0	0.0	36.6
Cn	2.4	12.4	29.6	46.1	46.1	65.7	96.3	0.8	9.9	0.0
Or	95.9	86.0	52.1	40.2	40.8	25.9	2.5	98.6	87.9	0.0

PR-1 is sample No.1 from the Padre Resource Ltd. property. PRBU is a sample of the barite-rich unit from the Padre Resource Ltd. property. NE-1 is sample No.1 from the Northern Eagle Mines Ltd. property. C denotes the grain core; m, the grain margin. All element oxides are in weight percent. FeO* is total iron content; nd: not detectable, Ab: albite, An: anorthite, Cn: celsian, Or: orthoclase.

operating conditions (15 kV, 10 nA, 2–5 μm beam diameter, 20-second counts, with synthetic glasses and minerals as standards). Mica polytypes were determined by X-ray diffraction with a Rigaku diffractometer (Cu$K\alpha$ radiation and quartz internal standard) and a Gandolfi camera (Cr$K\alpha$ radiation). Whole-rock analyses were carried out at the X-Ray Assay Laboratories, Don Mills, Ontario. Major element oxides and S were determined by X-ray fluorescence spectrometry (XRF), V, Ni, and Ag by directly coupled plasma spectrometry (DCP), the *REE*, along with Au, Sc, Cr, Co, Sb, As, Mo, Hf, Nb, Th, U and W, by instrumental neutron-activation analysis (INAA). The study of fluid inclusions was performed on a Linkam TH 600 programmable heating–cooling stage.

Petrography and Mineral Chemistry

Green mica schists from the study area contain feldspars, green mica, quartz, rutile, chromite, titanite, tourmaline, garnet, phlogopite, chlorite, and variable amounts of carbonates and sulfides. Fluorite is rare and is invariably restricted to cross-cutting veins. Feldspars and green mica, the most abundant minerals in green mica schists, have an antipathetic relationship in modal abundance, feldspars becoming more abundant toward the barite-rich unit.

Carbonates are not uncommon in all lithologies from the study area, and are particularly abundant in graphitic schists. In green mica schists, they occur in two textural varieties of distinct compositions: calcite (> 99 mol.% $CaCO_3$) in cross-cutting veins and ankerite [close to $Ca(Fe_{0.5}Mg_{0.5})(CO_3)_2$] in the rock matrix. Sulfides are locally very abundant (up to 30 vol.%) in the green mica schists, and generally occur as thin sulfide-rich layers (1–5 mm wide). Pyrite predominates, with minor amounts of sphalerite, chalcopyrite and pentlandite. It is noteworthy that there are at least two generations of pyrite in the green mica schists, as indicated by both textural evidence and color-staining with potassium permanganate (*cf.* Fleet *et al.* 1989).

Feldspars

There are two kinds of feldspar in the green mica schists from the study area; they belong to the alkali feldspar - hyalophane - celsian series and the plagioclase series. Plagioclase, invariably a minor constituent, is present in both cross-cutting veins and the rock matrix, but with a distinct composition: albite (An < 1%) in the former and oligoclase or andesine (An_{22} to An_{36}) with a minor amount of Sr (up to 0.4 wt.% SrO) in the latter. Members of the alkali feldspar - hyalophane - celsian series, on the other hand, are the most abundant minerals in the green mica schists, but celsian-predominant members are restricted to the barite-rich unit. All members of the alkali feldspar - hyalophane - celsian series generally occur as granoblastic mosaics in the quartzofeldspathic layers and are characterized by pronounced chemical zonation and, in contrast to some alkali feldspar grains from the Hemlo gold deposit (White & Barnett 1990), a general lack of twinning (Fig. 3a).

Representative compositions of the alkali feldspar - hyalophane - celsian series from green mica schists and the barite-rich unit are reported in Table 1 and are summarized on a celsian - orthoclase (microcline) - albite composition triangle (Fig. 4). They may be divided into three groups on the basis of occurrence and composition: (1) a Ba-rich feldspar (including celsian) in the barite-rich unit, (2) a ternary feldspar (hyalophane) in the green mica schist in direct contact with the barite-rich unit, and (3) a Ba-poor alkali feldspar (including microcline) in the green mica schist away from the barite-rich unit.

Chemical zonation in the Ba-rich feldspar from the barite-rich unit is characterized by a ternary (Ba–K–Na) core and a celsian-dominant margin. In general, the ternary (Ba–K–Na) core is chemically homogeneous and yet small, whereas the Ba-rich

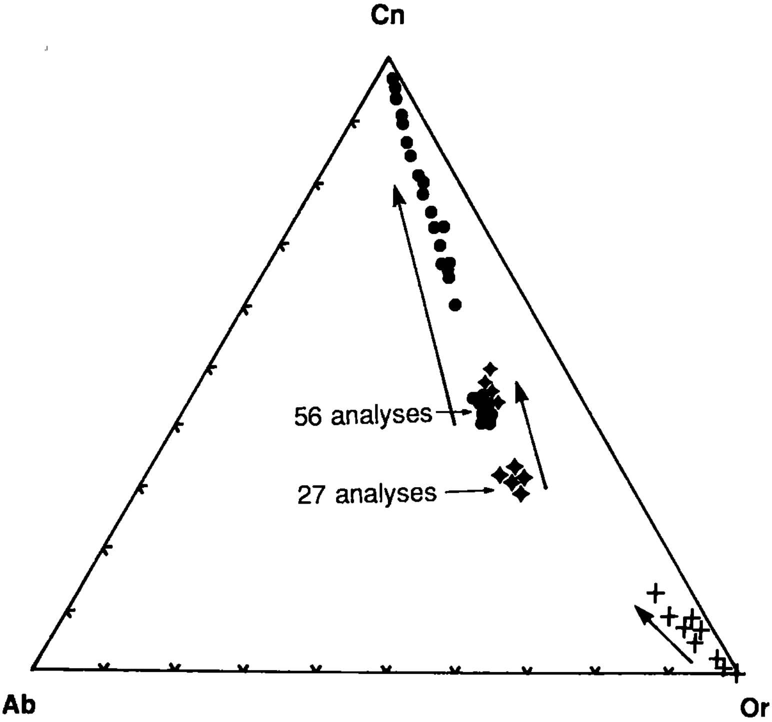

FIG. 4. Compositions of the alkali feldspar - hyalophane - celsian series in the celsian (Cn) - orthoclase (Or) - albite (Ab) composition triangle. Circles represent Ba-rich feldspars from the barite-rich unit, stars, ternary feldspars from green mica schists in direct contact with the barite-rich unit, and crosses, Ba-poor alkali feldspars from green mica schists away from the barite-rich unit. Arrows indicate compositional change from core to margin.

margin shows a gradational increase in Ba toward the grain boundary (Fig. 3a). However, complex zonations (oscillatory, sector, *etc.*) also are common in the margin. Strontium, which is typically low or absent in the celsian-dominant margin, may be significant (up to 0.5 wt.% SrO) in the ternary (Ba–K–Na) core. Locally, homogeneous grains of Ba-rich feldspar (close to end-member celsian in composition) may be present within the barite-rich unit (Fig. 3b).

The ternary feldspar (hyalophane) in the green mica schist in contact with the barite-rich unit is chemically zoned from a K–Ba–Na core to a Ba–K–Na margin. The compositional variation is very limited in both core and margin. The Ba–K–Na-bearing margin is compositionally similar to the core of the Ba-rich feldspar (Fig. 4, Table 1). Strontium is generally low in the margin of the ternary feldspar grains, but may reach 0.6 wt. % SrO in the core.

The Ba-poor alkali feldspar in the green mica schist away from the barite-rich unit also is chemically zoned, from a microcline-dominant core to a Ba-bearing margin, similar to the alkali feldspar in the Hemlo deposit (Harris 1989). The core of the Ba-poor alkali feldspar generally is homogeneous, whereas the margin shows a gradational increase in Ba toward grain boundaries. Interestingly, the absolute Ba content in this group of Ba-poor alkali feldspar varies in both margin and core, corresponding to the Ba abundance in the host rocks, and in some cases, the core of the Ba-poor alkali feldspar approaches the end-member composition ($KAlSi_3O_8$).

Gay & Roy (1968) investigated both synthetic and natural barian feldspars from different localities, and found that the synthetic high-temperature barian feldspars form a continuous solid-solution series. They postulated two miscibility gaps for the natural feldspars, one in the celsian-poor region (Cn_{10-30}) to account for the observed complex diffraction effects in single-crystal X-ray photographs, and the other in the celsian-rich region (Cn_{60-80}) on the basis of a compositional gap in the natural specimens. The analytical data (Fig. 4) for barian feldspar from the study area fall into four groups: (1) Cn_{0-15}, (2) Cn_{25-30}, (3) Cn_{40-47}, and (4) Cn_{65-96}, and show three compositional discontinuities. It is clear that compositions between Cn_{65} and Cn_{80} are not uncommon in the margin of the Ba-rich feldspar. The compositional discontinuity between core and margin in the Ba-rich feldspar is between Cn_{47} and Cn_{65}. A compositional gap between Cn_{40} and Cn_{55} has long been suggested on the basis of studies on natural specimens (Yosimura 1939, Vermaas 1953) and embraces the structural change from hyalophane to celsian. The Cn_{15-25} compositional gap is similar to the Cn_{10-30} gap postulated by Gay & Roy (1968). The Cn_{30-40} compositional gap corresponds directly to the chemical zonation between core and margin in the ternary feldspar and is less obvious than the other two compositional gaps (Fig. 4). It is not clear at this point whether the Cn_{30-40} compositional gap is a result of the limited data-base.

The compositions of the ternary feldspars from the study area are similar to those of Viswanathan & Brandt (1980) and Viswanathan & Kielhorn (1983a, b), except for the lack of a significant Fe^{3+} content. Viswanathan and coworkers also observed a disordered Al–Si distribution in the ternary (Ba–K–Na) feldspars from Otjosondu, Namibia, which are in close association with unmixed Ba-rich feldspar (celsian).

Green mica

Green mica, the most distinctive mineral and a major constituent (up to 40 vol.%) in the green mica schists, generally occurs as flakes oriented parallel or subparallel to schistosity. In places, aggregates of green mica replace chromite porphyroblasts and exhibit augen textures (Fig. 3c). Electron-microprobe analyses reveal that the green mica has a wide range of composition and is characterized by high concentrations of both Ba and Cr (up to 10.3 and 6.4 wt. % BaO and Cr_2O_3, respectively; Table 2). The compositional variation in the green mica exists not only in different grains but also is expressed in pronounced chemical zonation within grains (Fig. 3d). With rare exceptions, the chemical zonation in green mica involves both Ba and Cr, which commonly exhibit an antipathetic relationship: the core zone contains higher Cr and lower Ba than the margin. The contents of Ba and Cr in the green mica correlate well with the respective whole-rock abundances of these two elements. The maximum Ba content in green mica was obtained from green mica schists in direct contact with the barite-rich unit. Minor constituents in green mica from the study area include Mg, Fe and Na (up to 2.4 wt.% MgO, 1.3 wt.% FeO*, and 0.9 wt.% Na_2O). Vanadium, F, and Cl also were sought, but not detected. An X-ray-diffraction study indicates that the green mica possesses a $2M_1$ muscovite structure and, therefore, is a barian–chromian muscovite.

The level of titanium is characteristically high in most samples of barian-chromian muscovite from the study area (Table 2), particularly in grains in direct contact with rutile (Fig. 3e). Occasionally, green mica flakes along fractures in rutile contain up to 5.8 wt.% TiO_2 (Table 2). Unfortunately, an

TABLE 2. CHEMICAL COMPOSITION OF GREEN MICA

Sample	PR-1	PR-2c	PR-2m	PR-3c	PR-3m	PR-4c	PR-4m	NE-4	PR-5	NE-5
SiO_2	44.15	44.94	43.84	43.26	41.64	44.37	42.03	43.48	43.75	46.39
TiO_2	0.90	0.98	0.96	1.18	1.54	1.00	0.86	0.73	5.84	3.58
Al_2O_3	31.72	27.56	32.03	31.87	32.51	30.24	32.61	29.51	29.45	27.56
Cr_2O_3	2.38	4.75	1.00	1.46	1.65	1.36	0.63	6.39	3.36	4.32
FeO*	0.68	1.07	1.26	1.10	1.19	1.00	1.19	nd	0.23	0.30
MgO	1.55	2.34	2.37	2.00	2.06	2.04	2.06	1.88	2.24	3.11
MnO	nd	nd	nd	nd	nd	nd	nd	nd	nd	nd
CaO	0.05	nd	nd	0.02	nd	nd	nd	nd	nd	nd
BaO	3.64	6.42	8.44	7.46	10.19	7.79	10.31	4.16	3.07	3.04
Na_2O	0.67	0.27	0.36	0.29	0.26	0.40	0.30	0.72	0.68	0.76
K_2O	8.93	7.44	7.00	6.57	5.83	7.17	6.80	8.53	8.80	7.97
Total	94.67	95.77	97.26	95.21	96.88	95.37	96.79	95.40	97.43	97.03
chemical formulae calculated on the basis of 22 oxygen atoms										
Si	6.098	6.271	6.041	6.035	5.832	6.206	5.991	6.039	5.892	6.226
^{IV}Al	1.902	1.729	1.959	1.965	2.168	1.794	2.009	1.961	2.108	1.774
TET	8.000	8.000	8.000	8.000	8.000	8.000	8.000	8.000	8.000	8.000
^{VI}Al	3.261	2.803	3.242	3.274	3.197	3.295	3.291	2.869	2.566	2.585
Ti	0.093	0.103	0.099	0.124	0.162	0.107	0.090	0.076	0.591	0.361
Cr	0.260	0.524	0.109	0.161	0.183	0.153	0.066	0.702	0.358	0.458
Fe	0.079	0.125	0.145	0.128	0.139	0.107	0.125	0.000	0.026	0.034
Mg	0.319	0.487	0.487	0.416	0.430	0.435	0.432	0.389	0.450	0.622
Mn	0.000	0.000	0.000	0.000	0.000	0.000	0.000	0.000	0.000	0.000
OCT	4.013	4.042	4.082	4.103	4.112	4.097	4.004	4.036	3.990	4.060
Ca	0.007	0.000	0.000	0.003	0.000	0.000	0.000	0.000	0.000	0.000
Ba	0.197	0.351	0.456	0.408	0.559	0.441	0.573	0.226	0.162	0.160
Na	0.179	0.073	0.096	0.078	0.071	0.112	0.081	0.194	0.178	0.198
K	1.573	1.324	1.230	1.169	1.041	1.311	1.221	1.511	1.512	1.364
X	1.957	1.751	1.782	1.658	1.673	1.864	1.875	1.931	1.852	1.722

All element oxides are in weight percent. FeO* is total iron content; nd: not detectable.

X-ray study for this Ti-rich mica was not possible owing to its small size (< 15 μm wide).

Barium and Cr have long been known as minor constituents in muscovite from metamorphic rocks (Heinrich & Levinson 1955, Dunn 1984, Guidotti 1984, Rumyantseva *et al.* 1984, Treloar 1987a). Dymek *et al.* (1983) reported that green mica in the Archean Isua and Malene supracrustal rocks, southern West Greenland, possesses a 2*M* structure and contains up to 18 wt.% Cr_2O_3 and 8 wt.% BaO. Raase *et al.* (1983) also reported on green mica in Archean chromitiferous quartzites from Chitradurga, southern India, with 15 wt.% Cr_2O_3 and 8.5 wt.% BaO. Green muscovite from the study area is poorer in Cr but richer in Ba than its counterparts from Greenland and India.

Titanium also is a common minor constituent in metamorphic muscovite, and generally increases with an increase in metamorphic grade, but does not normally exceed 0.26 Ti atoms per 4 octahedral sites (*cf.* Cipriani *et al.* 1971, Guidotti 1984). The titaniferous barian–chromian muscovite from the study area contains up to 0.6 Ti atoms per 4 octahedral sites and therefore is unusual. High-Ti muscovite is generally associated with a Ti-saturated phase such as rutile or ilmenite (Cipriani *et al.* 1971, Guidotti 1984). The titaniferous barian–chromian muscovite from the study area is in direct contact with rutile. However, textural evidence indicates a replacement relationship of rutile by muscovite (Fig. 3e), rather than the equilibrium association observed in most metamorphic rocks.

Chromium and Ti in green mica from the study area appear to substitute for octahedrally coordinated Al, as indicated by a negative correlation between Cr and ^{VI}Al (Fig. 5a). Cr and Ti are mainly incorporated into the muscovite structure by the relationship (Mg + Fe) + Si = ^{IV}Al + (^{VI}Al + Cr + Ti) (Fig. 5b; *cf.* Guidotti 1984). The incorporation of Ba into green mica from the study area, however, must be independent of Cr and Ti, because the correlation between Cr and Ba is weak (Fig. 5c). The negative correlation between Ba and (K + Na) in green mica from the study area also is weak. However, the core-to-margin variations in Ba and (K + Na) within individual zoned muscovite grains are parallel or subparallel to the regression line for all data collected for muscovite from the study area (Fig. 5d).

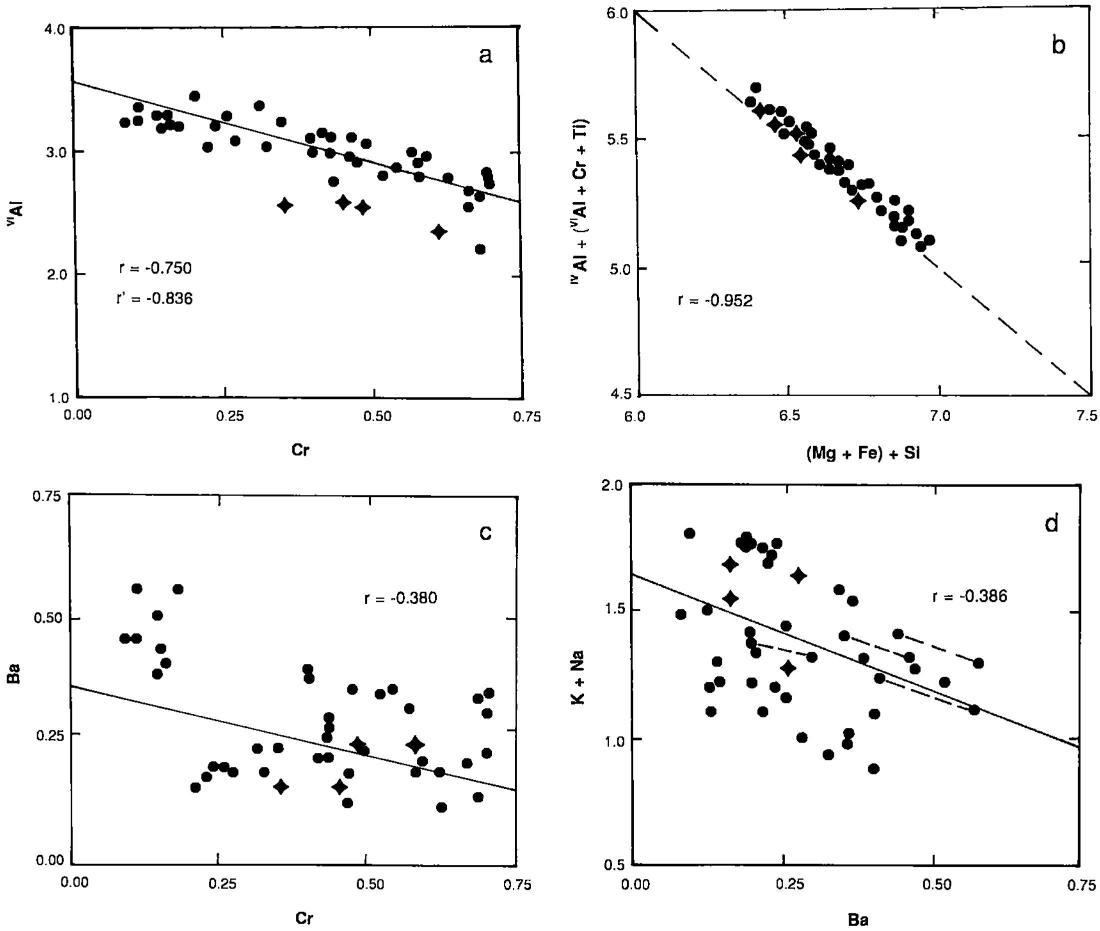

FIG. 5. Compositional variation in muscovite: a) ^{VI}Al *versus* Cr; b) ^{IV}Al + (^{VI}Al + Cr + Ti) *versus* (Mg + Fe) + Si; c) Ba *versus* Cr; and d) (K + Na) *versus* Ba. Circles represent barian–chromian muscovite, and stars, titaniferous barian–chromian muscovite. The solid lines are the result of a least-squares fit, the correlation coefficient *r* is calculated from all green mica compositions. The correlation coefficient *r'* between Cr and ^{VI}Al excludes Ti-rich compositions. The dashed lines in d represent core–margin variation.

TABLE 3. CHEMICAL COMPOSITION OF PHLOGOPITE, TOURMALINE, GARNET AND CHLORITE

Mineral	phlogopite			tourmaline			garnet		chlorite
Sample	PR-3	PR-5	PRBU	NE-2c	NE-2m	PR-2	PR-7	PR-8	NE-1
SiO_2	39.97	40.91	40.41	35.39	36.67	36.70	37.13	37.67	28.23
TiO_2	0.97	0.32	0.50	0.11	0.12	0.21	0.06	nd	nd
Al_2O_3	14.80	14.78	14.29	27.20	28.51	27.04	21.18	20.95	20.34
Cr_2O_3	1.84	1.06	0.14	9.82	6.87	7.33	0.19	nd	1.34
FeO*	7.00	0.48	nd	0.51	0.47	1.35	25.95	21.00	4.96
MgO	19.06	25.52	25.62	9.10	10.57	9.63	1.00	0.78	29.75
MnO	0.56	nd	nd	nd	nd	nd	7.30	15.88	nd
CaO	0.03	nd	nd	1.24	1.75	1.04	6.96	3.46	nd
BaO	2.56	1.39	3.68	nd	nd	nd	nd	nd	nd
Na_2O	0.11	0.29	0.26	2.08	1.86	2.34	nd	nd	nd
K_2O	8.31	8.95	8.73	nd	nd	0.03	nd	nd	nd
F	2.10	3.90	3.65	nd	nd	nd	nd	nd	nd
O = F	0.88	1.64	1.54	----	----	----	----	----	----
Total	96.44	95.96	95.79	85.63	86.82	85.69	99.77	99.74	84.62
Si	5.701	5.584	5.617	5.858	5.916	6.031	2.999	3.049	2.774
Al	2.487	2.410	2.393	5.305	5.418	5.235	2.016	1.997	2.354
Ti	0.104	0.033	0.052	0.014	0.015	0.026	0.004	0.000	0.000
Cr	0.207	0.114	0.015	1.285	0.876	0.952	0.020	0.000	0.104
Fe	0.835	0.050	0.000	0.071	0.000	0.000	1.752	1.423	0.407
Mg	4.050	5.192	5.308	2.246	0.063	0.186	0.122	0.094	4.358
Mn	0.068	0.000	0.000	0.000	2.542	2.360	0.500	1.088	0.000
Ca	0.005	0.000	0.000	0.220	0.000	0.000	0.650	0.301	0.000
Ba	0.144	0.074	0.200	0.000	0.303	0.186	0.000	0.000	0.000
Na	0.030	0.077	0.070	0.666	0.000	0.000	0.000	0.000	0.000
K	1.512	1.558	1.605	0.000	0.581	0.744	0.000	0.000	0.000
F	0.947	1.684	1.605	----	----	----	----	----	----
Oxygens	22.0	22.0	22.0	29.0	29.0	29.0	12.0	12.0	14.0

All element oxides are in weight percent. FeO* is total iron content; nd: not detectable.

Phlogopite

Phlogopite is present as a minor or trace constituent in all samples studied, including the barite-rich unit. It generally occurs as colorless, small flakes replacing plagioclase in quartzo-

TABLE 4. CHEMICAL COMPOSITIONS OF CHROMITE AND RUTILE

Mineral	chromite						rutile	
Sample	PR-2	PR-5c	PR-5m	NE-2	NE-3	NE-4	PR-5	NE-4
TiO_2	0.17	0.22	0.03	0.52	0.03	0.04	98.01	97.48
Al_2O_3	15.26	16.17	15.02	10.40	14.91	15.14	0.09	0.11
Cr_2O_3	49.22	49.64	50.61	53.71	50.41	49.95	2.04	1.54
FeO*	31.27	20.90	22.55	13.76	14.05	14.22	0.31	0.92
MgO	1.32	3.26	2.26	0.67	1.45	1.60	nd	nd
MnO	2.18	3.94	3.76	13.04	10.71	10.41	nd	nd
ZnO	0.54	5.94	5.82	6.94	8.67	8.89	nd	nd
Total	99.97	100.1	100.1	99.05	100.2	100.3	100.4	100.1
Chemical formulae calculated on the basis of 4 oxygen atoms								
Cr	1.337	1.330	1.375	1.521	1.379	1.362	0.043	0.032
Al	0.618	0.645	0.608	0.439	0.608	0.615	0.003	0.003
Fe^{3+}	0.041	0.020	0.016	0.026	0.013	0.022	0.000	0.000
Fe^{2+}	0.858	0.572	0.631	0.386	0.393	0.389	0.007	0.021
Ti	0.004	0.006	0.001	0.014	0.001	0.002	1.947	1.944
Mg	0.068	0.163	0.114	0.035	0.074	0.082	0.000	0.000
Mn	0.062	0.113	0.109	0.396	0.313	0.304	0.000	0.000
Zn	0.013	0.149	0.147	0.183	0.221	0.226	0.000	0.000
C/CA	0.68	0.67	0.69	0.78	0.69	0.69		
F/FM	0.93	0.78	0.85	0.92	0.84	0.83		

All element oxides are in weight percent. FeO* is total iron content. Fe^{3+} in chromite was estimated by charge-balance calculations; nd: not detectable; C/CA is the Cr/(Cr + Al) atomic ratio; F/FM is the Fe/(Fe + Mg) atomic ratio.

feldspathic layers, but it also is present as large plates of moderate pleochroism on foliation planes (Fig. 3f). The pleochroic phlogopite has lower values of the atomic ratio Mg/(Mg + Fe + Mn) (as low as 0.83); it approaches 1.0 in the colorless variety (Table 3). Similar to its dioctahedral counterpart, phlogopite also is characterized by high concentrations of Ba, Cr and Ti (up to 4.5 wt.% BaO, 2.3 wt.% Cr_2O_3, and 1.5 wt.% TiO_2). However, these constituents in phlogopite do not correlate with their respective bulk-rock abundances. Most interestingly, phlogopite is characterized by a high concentration of F (up to 3.9 wt. % F, equivalent to 1.76 F atoms per 4 volatile anions); the maximum F contents were encountered in the colorless variety (Table 3), perhaps as a result of Fe–F avoidance (Ekström 1972). An X-ray-diffraction study indicates that both colorless and pleochroic phlogopites from the study area consist of the 1*M* or 3*T* polytype.

Other minerals

Rutile, the most common oxide mineral in green mica schists, occurs as disseminated, idioblastic grains with a maximum dimension up to 0.3 mm. It is characterized by a minor amount of Cr (up to 2.0 wt.% Cr_2O_3; Table 4).

Chromite is not present in all samples of green mica schist, but is abundant in a few. Chromite

TABLE 5. WHOLE-ROCK COMPOSITIONS OF GREEN MICA SCHISTS AND ASSOCIATED ROCKS

Sample	PR-1	PR-2	PR-3	PR-4	PRBU	PR-20	PR-21	PR-22	PR-23	MTVL
SiO_2	47.9	49.3	53.7	54.9	39.1	69.6	48.5	65.9	67.1	45.40
TiO_2	0.61	0.71	0.84	0.85	0.48	0.56	0.63	0.58	0.61	0.97
Al_2O_3	11.1	12.2	15.4	17.0	9.68	8.62	11.4	9.78	10.1	11.7
Fe_2O_3*	10.9	18.1	11.2	8.15	4.68	9.67	10.2	10.1	9.22	18.8
MgO	3.77	1.11	1.13	1.47	0.76	1.09	3.71	1.27	1.42	7.49
MnO	0.15	0.07	0.07	0.09	0.04	0.08	0.15	0.07	0.14	0.67
CaO	6.38	1.29	1.22	1.78	1.99	<0.01	6.09	0.05	0.01	10.1
BaO	0.91	2.05	3.88	3.94	26.69	1.78	1.13	1.88	2.19	nd
Na_2O	1.14	3.87	3.90	4.68	1.92	0.20	1.15	0.25	0.25	1.13
K_2O	3.30	1.43	2.43	2.53	0.97	2.59	3.51	2.85	3.05	0.49
P_2O_5	0.05	0.04	0.03	0.04	0.11	0.04	0.06	0.05	0.05	0.09
LOI	13.5	9.93	6.08	4.70	3.62	4.54	13.4	6.0	4.54	1.39
Total	100.5	100.4	100.3	100.6	90.2	100.0	100.7	100.1	100.3	98.4
S	1.95	4.47	2.70	1.80	4.47	0.68	1.68	2.27	0.37	nd
As	2400	1900	2200	2700	59	1400	2200	3300	1900	14
Sb	160	1.6	2.0	1.2	3.5	49	94	21	14	0.8
Mo	<5	<5	<5	<5	18	140	<5	30	18	<5
Hg	27	18	14	<5	9	72	57	45	23	<5
Sc	52.5	45.6	64.6	45.6	11.6	24.0	48.6	31.3	40.6	62.7
V	200	220	330	280	76	190	230	190	28	270
Cr	4930	1920	2600	2740	290	8620	4720	9170	10900	410
Co	210	100	1400	160	23	26	170	210	13	67
Ni	1200	520	680	860	49	130	1100	1400	66	140
Hf	<1	2	<1	<1	17	<1	<1	<1	<1	3
Nb	10	16	<10	<10	69	<10	11	<10	<10	24
Th	4.5	0.7	nd	<0.5	2.3	<0.5	5.9	<0.5	<0.5	0.6
U	1.4	<0.5	nd	1.9	2.5	<0.5	2.9	<0.5	0.8	1.6
Zr	67	44	57	65	21	39	71	43	41	83
W	85	21	38	35	19	87	78	63	45	<3
Rb	89	50	71	83	19	45	92	52	54	16
Sr	95	381	501	667	1570	29	107	19	29	87
Al/Ti	18	17	19	20	20	15	18	17	17	12
Ti/Zr	55	96	88	77	137	86	53	81	89	70
Cr/Ni	4.1	3.7	3.8	3.2	5.9	66	4.3	6.6	165	2.9
Th/U	3.2				0.9		2.0			0.4

MTVL is a sample of garnet amphibolites. All oxides and S are in weight per cent; all trace elements, except Hg in parts per billion, are in parts per million. Fe_2O_3* is total iron content; LOI is loss on ignition.

generally occurs as porphyroblasts (up to 2 mm in diameter; Fig. 3c). Locally, chromite porphyroblasts (pseudomorphs) are completely replaced by aggregates of green mica. Minor amounts of discrete grains of chromite are found also in the rock matrix. Individual chromite grains are generally homogeneous, but a thin porous margin with slightly higher magnetite content is not uncommon in larger grains. Chemically, chromite in the green mica schists is characterized by very high concentrations of Mn and Zn (up to 13 wt.% MnO and 8.9 wt.% ZnO; Table 4) and, therefore, is a zincian-manganoan variety (*cf.* von Knorring *et al.* 1986, Pan & Fleet 1989). There is a positive correlation between Mn and Zn, both of which increase with a decrease in Fe and are considered to be a geochemical signature without any crystal-chemical significance.

Tourmaline, a rare mineral phase in green mica schists from the study area, occurs as deep green grains of dravite (up to 0.2 mm in maximum dimension) in close association with pyrite and green muscovite. A deep green core and light green margin are separated by a sharp boundary. The calculated formulae indicate that Cr substitutes for both Al and Mg in *Y* and *Z* sites, respectively (Table 3; *cf.* Dunn 1977). The absolute Cr content in tourmaline is considerably higher than that in the coexisting green muscovite.

Garnet is exceedingly rare in the green mica schists, and was recognized in two samples only. It occurs as sieve-textured poikiloblasts and is mainly composed of almandine component, with a considerable amount of Mn (up to 16 wt.% MnO, equivalent to 37 mol.% spessartine component) and minor Ca (Table 3).

Chlorite occurs in close association with pleochroic F-rich phlogopite along foliation planes and is characterized by a high Mg/(Mg + Fe + Mn) value (up to 0.92) and a minor Cr content (up to 1.3 wt.% Cr_2O_3; Table 3).

Titanite is a minor phase in green mica schists and generally occurs as disseminated, idioblastic grains in the rock matrix. Locally, very fine-grained aggregates of titanite appear to replace rutile porphyroblasts. However, there is no obvious difference in composition between the two textural varieties of titanite, which are both characterized by minor amounts of Al, Cr and Fe (< 1 wt.% of the respective oxides).

GEOCHEMISTRY

Whole-rock compositions were determined for eight samples of green mica schist, one of the structurally overlying mafic metavolcanic rock, and one of the barite-rich rock (Table 5). The good correlations that were noted between compositions of major mineral phases and whole-rock compositions are illustrated by Ba, which shows a systematic decrease in whole-rock content away from the barite-rich unit (Fig. 2), corresponding to a decrease in Ba content in both muscovite and feldspar. Similarly, the exceptionally high whole-

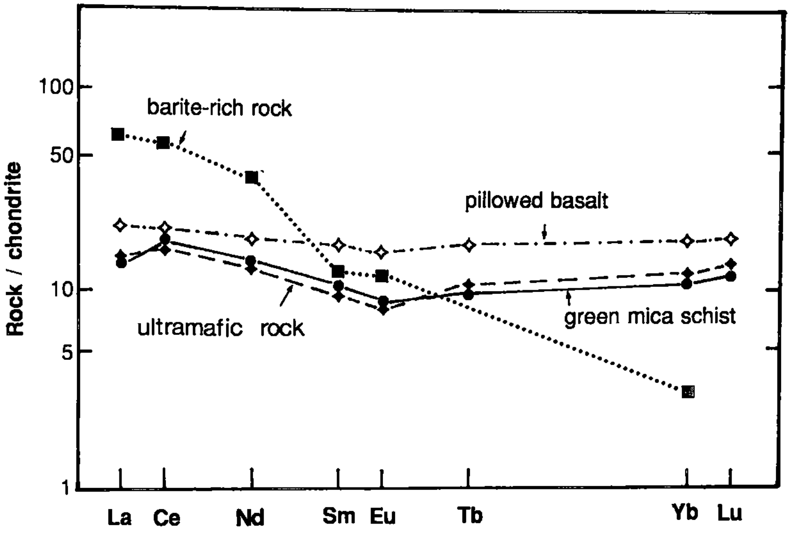

FIG. 6. Representative chondrite-normalized rare-earth-element (*REE*) patterns of green mica schists (circles) and barite-rich rocks (squares), compared with structurally overlying pillowed metabasalt (garnet amphibolite, open stars) and metamorphosed ultramafic rocks (tremolite–chlorite–talc schists, solid stars; data from Pan & Fleet 1988).

rock Cr concentrations (up to 10,900 ppm) correspond to the presence of chromite and high Cr content in muscovite and tourmaline. In addition, other transition metals, including Ni (up to 1400 ppm), V (330 ppm), and Co (210 ppm), also are characteristically enriched in the green mica schists.

Other elements notably enriched are As (up to 3300 ppm), Hg (72 ppb), Sb (160 ppm), Mo (140 ppm), W (87 ppm) and Sr (667 ppm). All of these anomalously high contents directly correlate with the mineralogy and abundance of sulfides, except for Sr, which appears to be positively correlated with Ba and attains 1570 ppm in the barite-rich unit (Table 5). The As in the green mica schists is mainly incorporated in the late generation of pyrite, as revealed by color-staining with potassium permanganate (*cf.* Fleet *et al.* 1989). This was confirmed by electron-microprobe analysis of pyrite.

The green mica schists are similar in some geochemical characteristics to mafic–ultramafic rocks of the region (*cf.* Pan & Fleet 1988), including the structurally overlying pillowed garnet amphibolites. This is illustrated by a uniform Al_2O_3/TiO_2 weight ratio of about 17 (σ = 0.7, n = 8) and a uniform Ti/Zr ratio of 78 (σ = 4.7, n = 8), and low Nb and Hf abundances in green mica schists (Table 5). Figure 6 shows a representative chondrite-normalized *REE* pattern of the green mica schists, which is characterized by low total *REE* abundances and low La_N/Yb_N (< 4), similar to those of metamorphosed ultramafic rocks from the study area and the structurally overlying mafic metavolcanic rocks (pillowed basalt). These findings suggest that the green mica schists from the study area have a mafic–ultramafic component (discussed below).

DISCUSSION

Petrographic and chemical evidence presented above show that the green mica schists from the study area probably formed according to the following paragenetic sequence: 1) chromite and rutile, 2) barian feldspar, barian–chromian muscovite, quartz, oligoclase–andesine, garnet, tourmaline, titanite, ankerite, first-generation pyrite, and sphalerite (the main mineral assemblage); 3) phlogopite, chlorite, titanite, quartz, albite, pyrite, fluorite and calcite.

At the White River property of LAC Minerals Ltd., 5 km east of the Hemlo deposit, Pan & Fleet (1989) reported the presence of zincian chromite coexisting with clinopyroxene and garnet. We considered the White River chromite to have crystallized immediately after the peak of regional thermal metamorphism (Pan & Fleet 1990). In the green mica schists of the study area, however, chromite is replaced by muscovite and, therefore, appears to predate the crystallization of the main mineral assemblage. It is unlikely to be a relict primary phase on the basis of its Mn- and Zn-rich composition (*cf.* Irvine 1967, von Knorring *et al.* 1986, Bernier 1990).

The concordance between the schistosity of the green mica schists and the penetrative foliation in all supracrustal rocks of the region indicates that the main mineral assemblage of the green mica schists formed broadly contemporaneously with regional thermal metamorphism. However, the main mineral assemblage itself does not provide constraints on the P–T–X conditions of its crystallization owing to a lack of well-calibrated geothermometers and geobarometers and the unusual compositions of the major mineral phases. A study of fluid inclusions in matrix quartz grains yielded homogenization temperatures of 530 ± 15°C, and indications of a dilute fluid (<2.5 wt.% NaCl equivalent; *cf.* Potter & Brown 1977, Potter *et al.* 1978). This is in good agreement with T estimates for the regional thermal metamorphism in the greenstone belt (Pan & Fleet 1990).

The restricted occurrence of green mica schists and the direct association of green barian–chromian muscovite with chromite (and rutile) imply that no significant remobilization of Cr (and Ti) occurred during this episode of metamorphic recrystallization. Patterns of mineralogical and chemical zonation in the green mica schists indicate that Ba was almost certainly introduced from the adjacent barite-rich unit during the crystallization of the main mineral assemblage. This Ba-metasomatism also was most likely protracted and progressive in nature, as indicated by complicated patterns of zonation and a progressive increase in Ba within individual grains of both feldspar and muscovite.

Dymek *et al.* (1983) discussed several possible sources for the elevated levels of Ba and Cr in micas and proposed a reaction of the type:

$$2\,BaSO_4 + FeCr_2O_4 = FeS_2 + 2\,BaO + Cr_2O_3 + 7/2O_2 \quad \text{barite + chromite = pyrite + ``mica''}$$

for the formation of barian–chromian muscovite in Isua and Malene supracrustal rocks of southern West Greenland. In the study area, Cr is readily available in pre-existing chromite, whereas Ba was introduced by a prominent synmetamorphic Ba-metasomatism from the adjacent barite-rich unit. Consistent with the proposal of Dymek *et al.* (1983), pyrite occurs in close association with barian–chromian muscovite, being locally abundant in the green mica schists. This reaction can include also the crystallization of a barian feldspar and Ti-bearing barian-chromian muscovite (by including rutile as an additional reactant) in the green mica schists of the study area. In addition, the local presence of sphalerite and spessartine-rich garnet as minor constituents in the green mica schists can be correlated with the elevated Zn and Mn contents in chromite. Therefore, the reaction of Dymek *et al.* (1983) contains almost all phases of the early and the main mineral assemblages observed in the green mica schists. It is unlikely that Ba was transported from the barite-rich unit to the green mica schists as $BaSO_4$, because of its low solubility in dilute solutions (Blount 1977). Dymek *et al.* (1983) suggested that the release of Ba from barite probably involved a metamorphic breakdown at conditions of elevated P–T. In the study area, the regional thermal metamorphism did reach middle-amphibolite facies. It is possible also that barium was released from barite by hydrothermal reactions.

Pan & Fleet (1990) demonstrated that skarns at the White River property formed during a major influx of hydrothermal fluids introduced along regional planar structures immediately after the peak of the regional thermal metamorphism, and suggested that the skarns were products of reactions between these hydrothermal fluids and mafic–ultramafic host rocks within or adjacent to the regional planar structures. It is conceivable that the main mineral assemblage in the green mica schists also is related to similar highly reactive hydrothermal fluids, and that the unusual mineral composition resulted from a combination of high concentrations of Cr and Ti in pre-existing chromite and rutile and a prominent episode of Ba-metasomatism from the adjacent barite-rich unit. This is strongly supported by the fact that the temperature of crystallization for the main mineral assemblage of the green mica schists is slightly lower than that of the peak of regional thermal metamorphism.

Phlogopite, chlorite, calcite, and other minerals in veins that cross-cut the penetrative foliation of the region seem to have crystallized later than the regional thermal metamorphism. A study of fluid inclusions in vein quartz grains yielded homogenization temperatures of 300–330°C, a fluid pressure of 1 kbar, and a fluid of moderate salinity ($<$ 10 wt.% NaCl equivalent; *cf.* Potter & Brown 1977, Potter *et al.* 1978). This range of conditions of crystallization and the typical mode of occurrence of these vein minerals are similar to the late, regional low- to very-low-grade alteration, which is generally characterized by abundant epidote–prehnite veins elsewhere in the Hemlo – Heron Bay greenstone belt (Pan & Fleet 1990). The paucity of calc-silicate minerals, such as epidote and prehnite, in the green mica schists of the study area is probably attributable more to high $X(CO_2)$ than to low activity of Ca (*cf.* Liou *et al.* 1983). A high $X(CO_2)$ during this late alteration is indicated by the local abundance of carbonates and is probably related to the closely associated graphitic schists.

Although the high levels of Ba in the green mica schists of the study area were almost certainly introduced from the barite-rich unit by a prominent Ba-metasomatism during the regional thermal metamorphism, there remains some uncertainty regarding the origin of the barite-rich unit itself. Patterson *et al.* (1983) suggested a sedimentary origin based on field relations and textural evidence. More recently, Cameron & Hattori (1987) proposed a model of hydrothermal mineralization based on sulfur isotope data for barite and pyrite. There is little doubt that this barite-rich unit existed prior to the formation of the main mineral assemblage in the green mica schists and that it served as the immediate source of Ba in these rocks.

Field relations do not provide unequivocal evidence for the origin of the high concentration of Cr in the green mica schists. Both sedimentary enrichment (*via* a heavy-mineral fraction or a clay-mineral fraction: Burns & Burns 1975, Treloar 1987b) and alteration of mafic–ultramafic volcanic rocks (Schreyer *et al.* 1981, von Knorring *et al.* 1986, Bernier 1990) must be considered, because the green mica schists are situated at a lithological boundary between mafic metavolcanic rocks and metasedimentary rocks (Figs. 1, 2). The first hypothesis can be discounted largely on geochemical grounds. Pan & Fleet (1990) reported that some cordierite–anthophyllite rocks associated with banded iron-formations (BIF) within a thick metasedimentary sequence at the White River property are metamorphosed Mg-, Fe-rich sediments, derived mainly from ultramafic components, and retain many sedimentary signatures, which are typically absent in the green mica schists from the study area. The second hypothesis is favored for several reasons. Firstly, it has been demonstrated above that the green mica schists show many remarkable similarities in geochemistry with metamorphosed mafic–ultramafic rocks (Fig. 6). Secondly, relict fragments of mafic–ultramafic rocks are locally present within the green mica schists. Thirdly, Pan & Fleet (1989, 1990) showed that the Cr-rich skarn at the White River property of LAC Minerals Ltd. was clearly derived from mafic–ultramafic host rocks within a regional-scale fracture zone during a phase of dilation. Brown *et al.* (1985) suggested that the barite-rich occurrences are situated within the regional-scale Heron Bay –

Black River fault zone. Therefore, it is conceivable that the high levels of Cr resulted from a selective enrichment of this element (Seyfried & Mottl 1982), along with Ti, during extensive hydrothermal alteration of mafic–ultramafic rocks within a regional-scale fault zone.

It may not be a coincidence that all three known occurrences of barian–chromian muscovite (Greenland, Dymek *et al.* 1983; India, Raase *et al.* 1983; and the study area), are situated in Archean terranes. On crystal-chemical grounds, Ba and Cr can readily substitute for K and Al, respectively, in the muscovite structure. The restricted occurrence of barian–chromian muscovite, therefore, is most likely related to adequate local sources of Ba and Cr. On a world-wide basis, barite occurrences and deposits (the usual source of Ba) occur in rocks of all ages, including Archean (Morse 1980). Ultramafic rocks (the ultimate source of Cr), however, are abundant only in Archean terranes. Therefore, micas enriched in both Ba and Cr may be restricted to Archean supracrustal rocks.

Finally, the green barian–chromian muscovite from the barite occurrences of the study area clearly is compositionally distinct from the vanadian muscovite that formed in the main ore-zone of the Hemlo gold deposit. Harris (1989) reported that the green mica of the Hemlo deposit contains a minor amount of Cr without detectable V. Analyses of four randomly selected green-mica-bearing samples from the Hemlo deposit by the present authors confirm only one sample of vanadian muscovite, whereas the remainder contain a minor amount of Cr ($<$ 1.0 wt.% Cr_2O_3), but no vanadium. Dymek *et al.* (1983) suggested that only a minor Cr content (probably less than 0.1 wt.% Cr_2O_3) is required to impart the characteristic emerald green color in muscovite. Schmetzer (1982) reported that the optical absorption bands due to V^{3+} in silicates are very close to those of Cr^{3+} and, consequently, the color of a particular mineral is commonly the same regardless of whether the chromophore is Cr^{3+} or V^{3+}.

ACKNOWLEDGEMENTS

We thank R. Thorpe, J.L. Walshe, and an unidentified referee for constructive reviews and R.F. Martin and C.M. Lesher for editorial assistance. We also thank J. Gray, W.E. Stone, M. Smyk and T.L. Muir for assistance in the field, J. Forth for the preparation of polished thin sections, Y. Cheng for assistance with X-ray diffraction, and R.L. Barnett and D.M. Kingston for assistance with electron-microprobe analyses and fluid inclusion techniques. This study was supported by an Ontario Geological Survey Geoscience Research Grant (No. 393) to M.E.F.

REFERENCES

BERNIER, L.R. (1990): Vanadiferous zincian–chromian hercynite in a metamorphosed basalt-hosted alteration zone, Atik Lake, Manitoba. *Can. Mineral.* **28**, 37-50.

BLOUNT, C.W. (1977): Barite solubilities and thermodynamic quantities up to 300°C and 1400 bars. *Am. Mineral.* **62**, 942-957.

BROWN, P., CARSON, D., COOPER, P., FARR, E., GIBSON, J., HARVEY, J., HOGG, W., MACISAAC, N., MACKIE, B., NASH, W. & PIERCE, G. (1985): Golden Giant joint venture properties - Hemlo. *In* Gold and Copper–Zinc Metallogeny within Metamorphosed Greenstone Terrain, Hemlo - Manitouwadge - Winston Lake, Ontario, Canada. *Geol. Assoc. Can. - Can. Inst. Min. Metall.* (R.H. McMillan & D.J. Robinson, eds.), 58-65.

BURNS, V.M. & BURNS, R.G. (1975): Mineralogy of chromium. *Geochim. Cosmochim. Acta* **39**, 903-910.

CAMERON, E.M. & HATTORI, K. (1985): The Hemlo gold deposit, Ontario: a geochemical and isotopic study. *Geochim. Cosmochim. Acta* **49**, 2041-2050.

_____ & _____ (1987): Archean sulphur cycle: evidence from sulphate minerals and isotopically fractionated sulphides in Superior Province, Canada. *Chem. Geol.* **65**, 341-358.

CIPRIANI, C., SASSI, F.P. & SCOLARI, A. (1971): Metamorphic white micas: definition of paragenetic fields. *Schweiz. Mineral. Petrogr. Mitt.* **51**, 259-302.

CORFU, F. & MUIR, T.L. (1989a): The Hemlo - Heron Bay greenstone belt and Hemlo Au–Mo deposit, Superior Province, Ontario, Canada. 1. Sequence of igneous activity determined by zircon U–Pb geochronology. *Chem. Geol.* **79**, 183-200.

_____ & _____ (1989b): The Hemlo - Heron Bay greenstone belt and Hemlo Au–Mo deposit, Superior Province, Ontario, Canada. 2. Timing of metamorphism, alteration and Au mineralized from titanite, rutile and monazite U–Pb geochronology. *Chem. Geol.* **79**, 201-223.

DUNN, P.J. (1977): Chromium in dravite. *Mineral. Mag.* **41**, 408-410.

_____ (1984): Barian muscovite from Franklin, New Jersey. *Mineral. Mag.* **48**, 562-563.

DYMEK, R.F., BOAK, J.L. & KERR, M.T. (1983): Green micas in the Archean Isua and Malene supracrustal rocks, southern Western Greenland, and the occurrence of a barian–chromian muscovite. *Rapp. Grønlands Geol. Unders.* **112**, 71-82.

EKSTRÖM, T.K. (1972): The distribution of fluorine among some coexisting minerals. *Contrib. Mineral. Petrol.* **34**, 192-200.

FLEET, M.E., MACLEAN, P.J. & BARBIER, J. (1989): Oscillatory-zoned As-bearing pyrite from strata-bound and stratiform gold deposits: an indicator of ore fluid evolution. *Econ. Geol., Monograph* **6**, 356-362.

GAY, P. & ROY, N.N. (1968): The mineralogy of the potassium-barian feldspar series. III. Subsolidus relationships. *Mineral. Mag.* **36**, 914-932.

GOAD, R.E. (1987): *The Geology, Primary and Secondary Chemical Dispersion of the Hemlo Au District Metal Occurrences, Northwestern Ontario.* M.Sc. thesis, Univ. Western Ontario, London, Ontario.

GRAHAM, C.M. & POWELL, R. (1984): A garnet-hornblende geothermometer: calibration, testing, and application to the Pelona schist, southern California. *J. Metamorph. Geol.* **2**, 13-31.

GUIDOTTI, C.V. (1984): Micas in metamorphic rocks. *In* Micas (S.W. Bailey. ed.). *Rev. Mineral.* **13**, 357-467.

HARRIS, D.C. (1989): Mineralogy and geochemistry of the Hemlo gold deposit, Ontario. *Geol. Surv. Can., Econ. Geol. Rep.* **38**.

HEINRICH, E.W. & LEVINSON, A.A. (1955): Studies in the mica group; X-ray data on roscoelite and barium-muscovite. *Am. J. Sci.* **253**, 39-43.

KOHN, M.J. & SPEAR, F.S. (1990): Two new geobarometers for garnet amphibolites, with application to southern Vermont. *Am. Mineral.* **75**, 89-96.

IRVINE, T.N. (1967): Chromian spinel as a petrogenetic indicator. 2. Petrologic applications. *Can. J. Earth Sci.* **4**, 71-103.

LIOU, J.G., KIM, H.S. & MARUYAMA, S. (1983): Prehnite-epidote equilibria and their petrologic applications. *J. Petrol.* **24**, 321-342.

MACDONALD, A.J. (1986): *Proceedings of Gold'86, an International Symposium on the Geology of Gold* (Toronto, 1986). Konsult Intern. Inc., Willowdale, Ontario.

MORSE, D.E. (1980): Barite. *In* Mineral Facts and Problems. *U.S. Bureau of Mines, Bull.* **671**.

MUIR, T.L. (1982a): Geology of the Hemlo area, district of Thunder Bay. *Ont. Geol. Surv., Rep.* **217**.

______ (1982b): Geology of the Heron Bay area, district of Thunder Bay. *Ont. Geol. Surv., Rep.* **218**.

______ & ELLIOTT, A.G. (1987): Hemlo tectonic-stratigraphic study, district of Thunder Bay. *Ont. Geol. Surv., Misc. Pap.* **137**, 117-129.

PAN, YUANMING & FLEET, M.E. (1988): Metamorphic petrology of the White River property of the LAC Minerals Ltd., Hemlo area. *Ont. Geol. Surv., Misc. Pap.* **140**, 164-176.

______ & ______ (1989): Cr-rich calc-silicates from the Hemlo area, Ontario. *Can. Mineral.* **27**, 565-577.

______ & ______ (1990): Metamorphism, geochemistry, skarn development and gold mineralization in the White River gold prospect, Hemlo area. *Ont. Geol. Surv., Misc. Pap.* **150**, 13-26.

PATTERSON, G.C., MASON, J.K. & SCHNIEDERS, B.R. (1983): Report of activities 1983. Thunder Bay resident geologist area, north central region. *Ont. Geol. Surv. Misc. Pap.* **117**, 47-106.

POTTER, R.W., II & BROWN, D.L. (1977): The volumetric properties of aqueous sodium chloride solutions from 0 to 500°C at pressures up to 2000 bars based on a regression of available data in the literature. *U.S. Geol. Surv., Bull.* **1421-C**.

______, CLYNNE, M.A. & BROWN, D.L. (1978): Freezing point depression of aqueous sodium chloride solutions. *Econ. Geol.* **73**, 284-285.

RAASE, P., RAITH, M., ACKERMAND, D., VISWANATHAN, M.N. & LAL, R.K. (1983): Mineralogy of chromitiferous quartzites from south India. *J. Geol. Soc. India* **24**, 502-521.

ROACH, D.E., CAMERON, E.M. & HATTORI, K. (1986): Geology and geochemistry of baritic bodies west of Hemlo. *Geol. Assoc. Can. - Mineral. Assoc. Can. - Can. Geophys. Union, Program Abstr.* **11**, 119-120.

RUMYANTSEVA, E.V., MISHEHENKO, K.S. & KALINICHEVA, L.L. (1984): Taeniolite and chromian-vanadian micas in metasomatites of Karelia. *Zap. Vses. Mineral. Obshchest.* **113**, 68-75 (in Russ.).

SCHMETZER, K. (1982): Absorption spectroscopy and colour of vanadium(3+)-bearing natural oxides and silicates - a contribution to the crystal chemistry of vanadium. *Neues Jahrb. Mineral. Abh.* **144**, 73-106.

SCHREYER, W., WERDING, G. & ABRAHAM, K. (1981): Corundum-fuchsite rocks in greenstone belts of southern Africa: petrology, geochemistry and possible origin. *J. Petrol.* **22**, 191-231.

SEYFRIED, W.E., Jr. & MOTTL, M.J. (1982): Hydrothermal alteration of basalt by seawater under seawater-dominated conditions. *Geochim. Cosmochim. Acta* **46**, 985-1002.

TRELOAR, P.J. (1987a): Chromian muscovites and epidotes from Outokumpu, Finland. *Mineral. Mag.* **51**, 593-599.

______ (1987b): The Cr-minerals of Outokumpu - their chemistry and significance. *J. Petrol.* **28**, 867-886.

VERMAAS, F.H.S. (1953): A new occurrence of barian feldspar at Otjosondu, South-West Africa, and an X-ray method for determining the composition of hyalophane. *Am. Mineral.* **38**, 845-857.

VISWANATHAN, K. & BRANDT, K. (1980): The crystal structure of a ternary (Ba,K,Na)-feldspar and its significance. *Am. Mineral.* **65**, 472-476.

______ & KIELHORN, H.-M. (1983a): Variations in the chemical compositions and lattice dimensions of (Ba,K,Na)-feldspars from Otjosondu, Namibia and their significance. *Am. Mineral.* **68**, 112-121.

______ & ______ (1983b): Al, Si distribution in a ternary (Ba,K,Na)-feldspar as determined by crystal structure refinement. *Am. Mineral.* **68**, 122-124.

VON KNORRING, O., CONDLIFFE, E. & TONG, Y.L. (1986): Some mineralogical and geochemical aspects of chromium-bearing skarn minerals from northern Karelia, Finland. *Bull. Geol. Surv. Finland* **58**, 277-292.

WHITE, J.C. & BARNETT, R.L. (1990): Microstructural signatures and glide twins in microcline, Hemlo, Ontario. *Can. Mineral.* **28**, 757-769.

YOSIMURA, T. (1939): Studies on the minerals from the manganese deposit of the Kaso mine, Japan. *J. Fac. Sci., Hokkaido. Univ.*, ser. **4**, 313-380.

Received September 17, 1990, revised manuscript accepted January 9, 1991.